International Journal of Science and Research (IJSR)
ISSN: 2319-7064
Impact Factor (2018): 7.426

Structural and Tectonic Subsidence History Study of Southwestern Sirt Basin, Libya

Mohamed Saleem

Exploration Research Department, Libyan Petroleum Institute, Tarabulus, Libya

Abstract: ***The study area is the south most of the western part of the Sirt Basin. Seismic and gravity data have been used to delineate the local structures within the area of study and to investigate their lateral and vertical extension. The area is located nearby Al-Harouge basaltic mountain which associated with a number of ingenious intrusions. The seismic data show that the area dominated by a group of differentiated fault zones caused the common characteristics of the area. The majorities of these faults are trending NW-SE coincidences with the general tectonic elements of the basin, and extremely controlled the strata thickness and formed a number of deep sub-troughs. Group of wells was used to study the tectonic history of the area the analysis shows that the area passed with four main tectonic stages, the first stage was the initial rift phase, started proximately at the Mid-Cretaceous time ~100Ma during which the area underwent a significant amount of subsidence, the second stage began at the ~84Ma and characterized by a slow post-rift subsidence persisted until the second rift phase initiated during which a rapid syn-rift subsidence took place and continued through the Paleocene–Eocene time. At about 40Ma the second post-rift subsidence was begun and persisted to the present day.***

Keywords: Rift, Tectonic subsidence, seismic interpretation, Sirt Basin, Zallah Trough

1. Introduction

Numerous of studies have been published about the tectonic history of the Sirt Basin and the configuration of the related regional structures, but in spite of these wealthy there are some areas within the basin still need more investigation and focused detailed tectonic studied, one of these areas is the south most of the western part of the basin. The study area is located in the southwestern part of Sirt Basin central north Libya, between the longitudes 18° 20′ And 19° 20′ East and latitudes 27° 30′ And 28° 00′ North, most of the area located in Zallah Trough and the eastern part is located within Dahrah- Hofrah platform figure (1-a).

Good coverage of seismic data, about fifty of 2D-lines and three volumes of 3D seismic data figure-(1-b), in an addition to the borehole data have been used to delineate the local structures within this area of study and to track their lateral and vertical extension.

2. Literature Survey

The Sirt Basin is one of the youngest inland basins with Paleogene and Neogene exposures; the basin consists of a series of grabens and horsts tectonics, some of which are delineated by surface mapping. To the E and SE of the Sirt Basin lies a depression with eolian sand often referred to as the "Great Sand Sea" or the "Libyan Desert". Below this relatively thin veneer of sand lies a complex subsurface ranging from Paleozoic to Neogene in age. During the early Paleozoic (Cambrian), the continental siliciclastic deposition was predominate most of the North Africa from Morocco to the Middle East, and during Ordovician and Silurian, the environment of depositions was marginal marine to marine (Hammuda et al, 1985). Due to the late Silurian major event (Caledonian Orogeny) uplift and erosion, the Paleozoic basins in Libya are limited. The major trends, such as the Sirt-Tibisti arch that trending north-south and separating the Kufrah

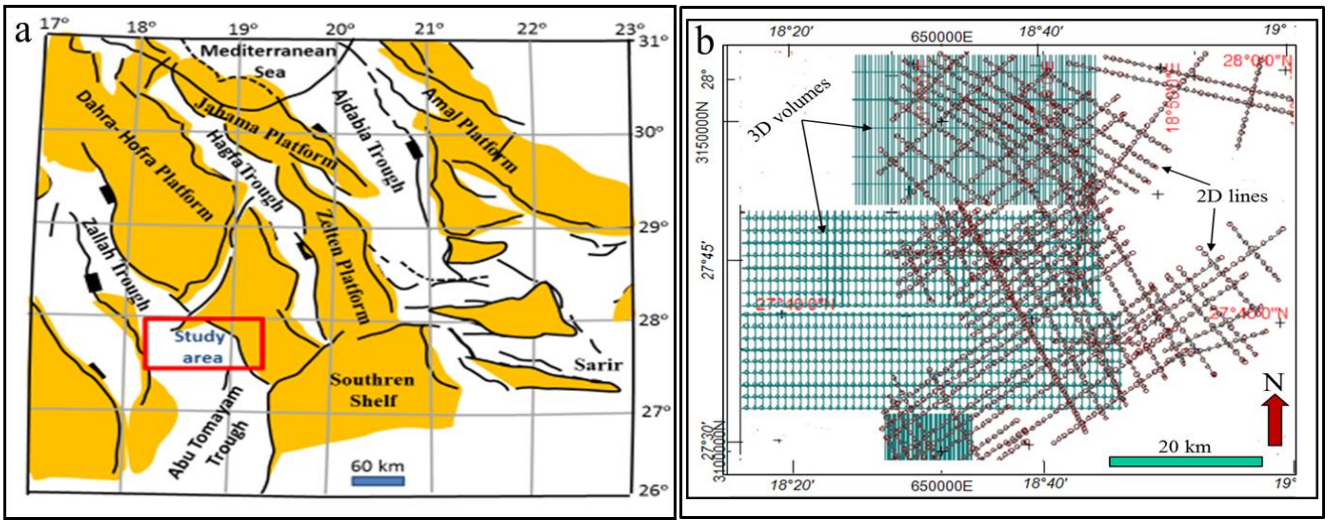

Figure 1: (a) location of the study area and the adjacent structural elements of Sirt Basin, (b) the coverage of the seismic data

Licensed Under Creative Commons Attribution CC BY

and eastern basins from the Murzuq Basin and Ghadamis Basin in the west, and the Gargaf Arch that extending east-west between the Ghadamis Basin and Murzuq Basin, were created during the Hercynian orogeny (Klitzsch, 1971).

The characteristics of the abundance Ordovician glacial and periglacial rocks in Libya and Algeria extremely supports the suggestion said that the western Gondwana was too close to the South Pole at that time, (Benchley et al., 1994). The major source rocks of the hydrocarbon accumulation in North Africa were performed after the marine transgression, during the Silurian time marine deposition which produced a thick sequence of a black shale that formed major source rocks (Luning et al., 2000).

The Akakus Formation overlying the early Silurian black shales in Libya consists of pro-delta and delta sediments. Four transgressive sequences resulted due Western Gondwana rifting and crustal separation that finally produced the dominated Early Devonian sediments in Libya then a large scale of deltaic deposition took place by the mid-Devonian, which was ultimately uplifted and eroded. During the mid-late Devonian, the northwestern margin of Gondwana collided with Laurasia (Hallett, 2002). The compressional tectonics (Hercynian Orogeny) during Late Carboniferous uplifted and eroded both the whole widely distributed Devonian marine siliciclastic rocks and the early Carboniferous marine- continental deposition in Libya, the major trends such as the Gargaf Arch, Jefarah uplift, and Sirt-Tibisti arch were performed and subsequently formed the Paleozoic basin margins (Luning et al., 2000).

Most of these new trends created from the old regional tectonic structures such as the former Kalanshiyu Trough produced the Sirt Arch by the inversion and subsequent deep erosion events. The Qarqaf Arch was resulting in the detachment of the Ghadamis Basin from the Murzuq Basin. Thus, all these structures events were resulted by the superposition of Hercynian trends upon the Lower Paleozoic trends.

Most of Libyan region was exposed by mid-late Carboniferous time, and a major marine regression dominated the North Africa, that led to erosion and terrestrial deposition (De Wit et al., 1988). The Permian rifting subsequently extended from the Tethys gulf toward the west along the suture line of the Gondwana-Laurasia (Ricou 1994, Hallett 2002).

2.1 Mesozoic events

During the Triassic the Pangaea break-up started when an extension and crustal thinning predominated the North African continental margin. By the late Triassic the incipient break-up had spread into the West and East parts of former Gondwana, coupled the African eastern margin rifting with the southern margin of the Arabian plate (Morgan et al., 1998). Onshore and offshore Libya are represent the Triassic extensional fault systems, which are distenguished by a number of unconformities. The Triassic deposition took place first in the Libyan offshore basins and then into the Nafusah Uplift, which formed the Tethyan shoreline, whereas Triassic terrestrial sedimentation dominated the rest of Libya (Wilson and Guiraud, 1998). Wilson and Guiraud (1998), stated that the Triassic sediments in eastern Libya may be deposited in incipient syn-rift grabens.

Dercourt et al. (1986) estimated the eastward displacement of Africa during the early Cretaceous to be about 2.5cm/year. Such movement of Africa caused a stretching and collapsing of Sirt Arch in the mid-Cretaceous took place. Meantime, the northern margin of the African plate tilted seaward. The Sirt Basin was has been formed from the remains of the northern part of the collapsed Sirt Arch into five major grabens (Hameimat, Ajdabiyah, Maradah, Zallah and Hun), isolated by four major platforms (Amal-Jalu, Zeltan, Zahrah-Bayda, and Waddan). These major tectonic structures generally oriented north-northwest–south-southeast. In the Late Cretaceous and Paleocene, the Sirt Basin kept the same structural construction throughout the recurrent episodes of faulting (Barr and Weegar, 1972; Gumati and Kanes, 1985; Baird et al., 1996).

In some troughs in the Sirt Basin such as the Hameimat and Sarir Troughs there is an evidence of subsidence and pull-apart that took place during the Neocomian and Barremian, and the continental sands covered a widely area which produced one of the most generous hydrocarbon reservoirs in the province. The sediments of the early Cretaceous restricted to the northern margin of Libya. In the late Cretaceous, again the extension became dominant along the southern margin of the Tethys, and the shallow marine carbonate sediments covered most of the Sirt Basin horsts, by the end of Cretaceous, some of these carbonate sediments performed significant hydrocarbon reservoirs, and simultaneously the grabens totally infilled (Guiraud, 1998; Boote et al., 1998).

2.2 Cenozoic Events

In western Libya the early Cenozoic time characterized by the Uplift and marine regression, while in the Sirt Basin a gentle subsidence took place in the earlier Cretaceous grabens. Major subsidence continued in the Ajdabiyah Trough. The Paleocene and Eocene carbonates formed the major carbonate hydrocarbon reservoirs in Libya (Hallett, 2002). In the Hun Graben Subsidence occurred during Priabonian to Burdigalian times. This period was characterized by the direction change of Africa movement toward the northwest (Dercourt et al., 1986). Since the end of the Oligocene a number of great changes have occurred in the western Mediterranean. In the Sirt Basin tilting towards the ENE, gentle folding, and subsidence were the main events at that time, while on the Medina and Sirt Wrenches offshore the events were represented in the dextral wrenching (Anketell, 1996).

A rate of ~1.0 cm/ year of a northeastward drift of Africa has persisted Since the Tortonian. While a huge rise in salinity characterized the Messinian time, when the drop of the Mediterranean sea level exceeds 500 m, and huge thick evaporites were deposited in the deep basins of Mediterranean. The presence of the buried deep valleys near to Ajdabiyah Trough confirmed the drop of the base-level in the Messinian time which exceeds 500 m below the present day sea level (Barr and Walker, 1973; Hallett, 2002).

Licensed Under Creative Commons Attribution CC BY

3. Seismic Interpretation

Number of interesting reflectors has been picked from both 2D and 3D seismic data, the interpretation reveals that there are three interesting aspects in the study area, on which the analyses will be focused:

I) the most important one is the Barrut structure in the northern part of Area (figure-2). G1a-72 is the nearest well that was drilled in 1967 to evaluate the reservoir within this structure which was appearing in a 2D data as a large high relief four-way dip closed structure.

The uppermost continues horizon has been interpreted was the top of Gialo Formation (top Upper Eocene) which represent the main reservoir in the Gialo field. The time structure map of this horizon is clearly demonstrate the structure and shows that it is elongated WSW-ENE and it is highly faulted and segmented by a group of major and minor normal and ramp faults striking NW-SE and dipping NE forming a semi narrow graben in the central area of the structure. The crest of the structure is rising about 0.25sec relative to the bounded area (figure-2 & figure-3).

The defining narrow graben, itself nearly segmented the structure into two sub-structures north and south labelled on the map by A and B, with approximately covered areas ~180 km^2 and 148 km^2 respectively. The south portion (A) represents the footwall of the fault zone-1 which consists of large number of parallel to sub-parallel normal faults producing a total heave of ~1.0 km, and an ultimate throw as 0.3 sec (~840 m), this fault zone is one of several fault zones dominated the study area as will be shown later.

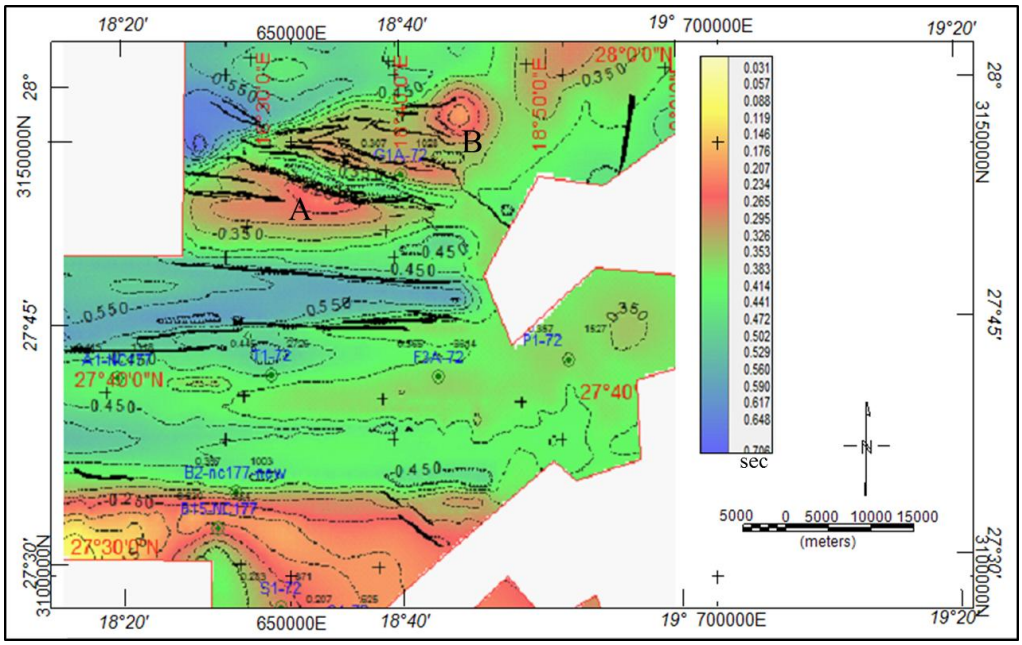

Figure 2: Time structure map created by 3D seismic data for the top Gialo Formation (top U. Eocene), the map is clearly demonstrate the Barrut Arch in the northern part which is highly impacted by NW-SE extension faults

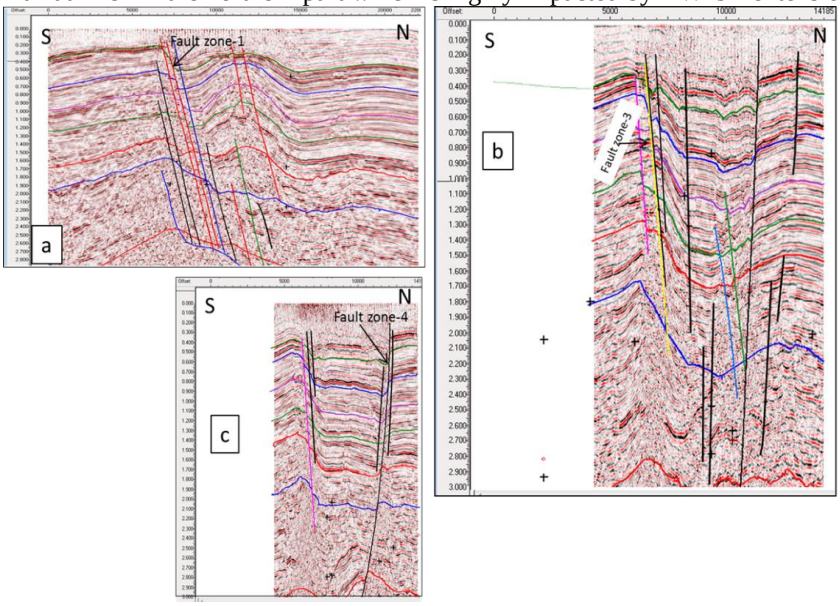

Figure 3: Interpreted seismic profiles showing the fault zones that dominated the area, (a) from the northern volume of 3D seismic data, (b) and (c) from the middle volume.

Licensed Under Creative Commons Attribution CC BY

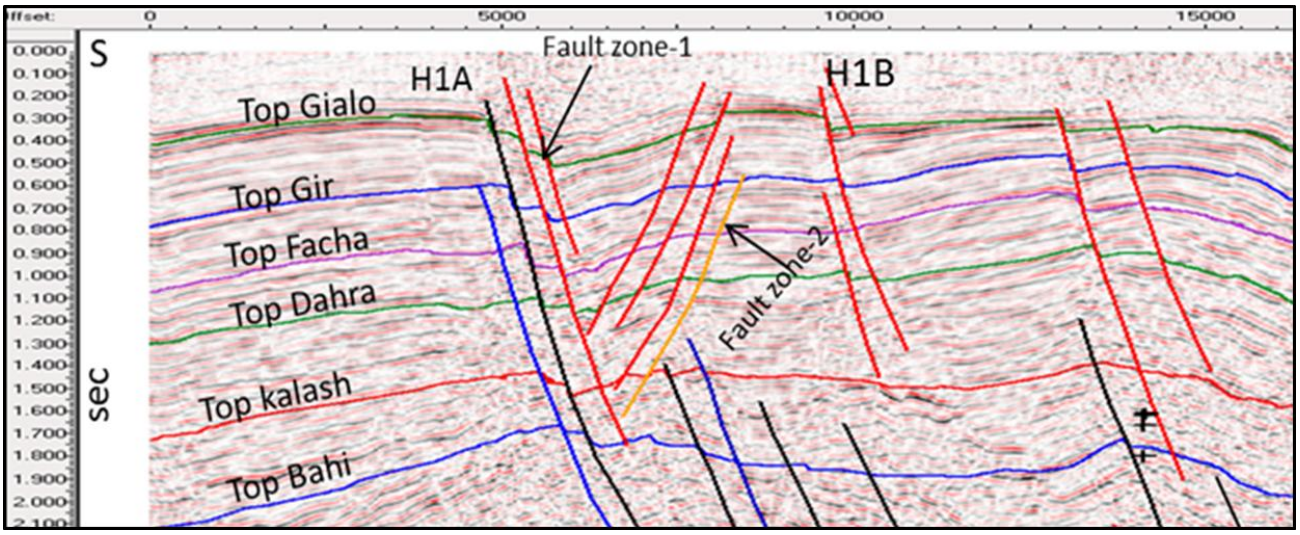

Figure 4: One of the interpreted seismic lines from 3D volume, the line Travers the barutt structure trun

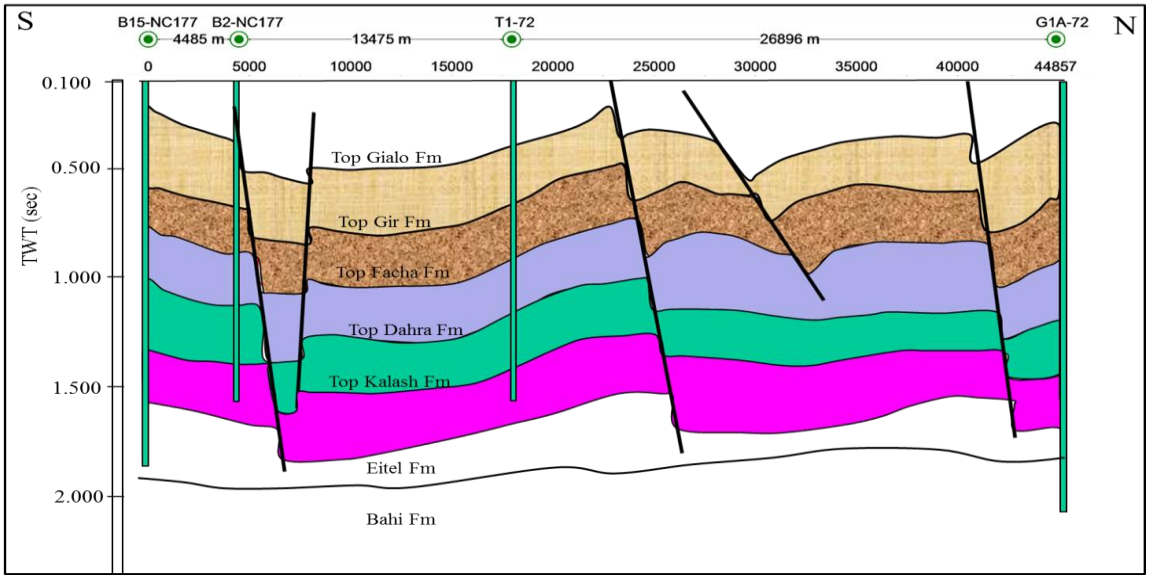

Figure 5: Interpreted N-S regional seismic line (~ 45 km), demonstrate the regional tectonics in the study area

The most faults within fault-zone-1 are younger than the Mid-Eocene in age, since they started above the Gialo Formation (Mid-Eocene) and terminate in the Upper Cretaceous depositional package; others are truncated by the antihiatic faults and terminated shallower at the Lower Paleocene. The interpreted arch (Barrut Arch) is a natural barrier separates Abu Tumayam Trough in the south from the Zallah Trough in the north.

the hanging wall of the fault zone-1 is clearly demonstrate the rollover anticline form, which impacted by a group of antithetic southward dipping faults that forming the fault zone-2 (Figure-4), with a cumulative heave and throw about 125 m and 0.058 sec (~162 m) respectively. These faults have impacted the depositional units of Paleocene, and lower and Mid-Eocene, however the seismic data does not obviously show any evidence confirm that these faults were active during the Cretaceous stage of rifting, which suggesting that their initiation age not early than the late Eocene.

Licensed Under Creative Commons Attribution CC BY

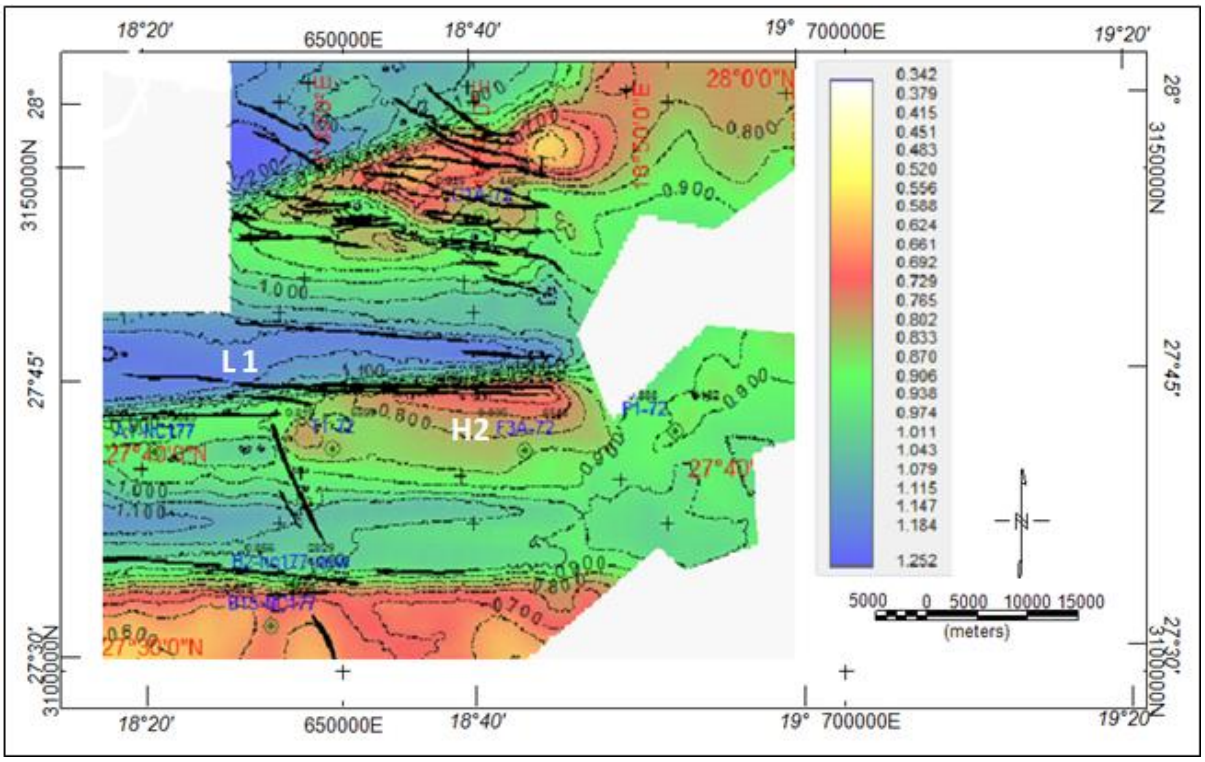

Figure 6: TWT structure map of the Top Facha Member (lower Eocene), the south part HA of the structural high started to disappear while the north part HB still clear demonstrated. The grabens (L2 and L3) slightly dip westward.

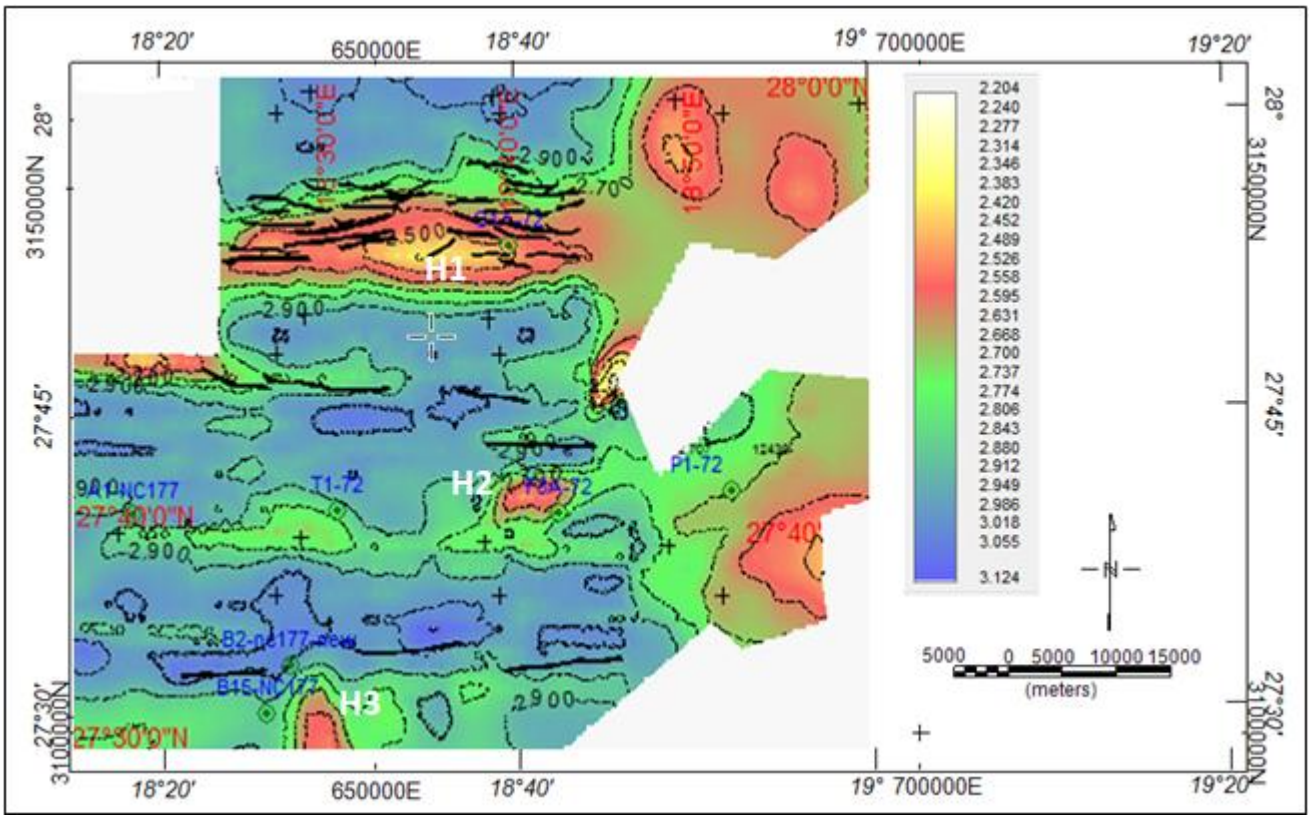

Figure 7: Time structure map of the top Precambrian basement, the northern prominent high structure, Barrut Arch (H1) tilted to be east-west extending, the south structural high (H3) is still dominant at the basement depth, several parallel to sub-parallel WNW-ESE faults crosscut the arch, the contour interval is (0.1 sec)

II) The second high structure is located further to the south centred at 27 45N and 18 40 E, although this structure in not clear enough at the previous interpreted shallow surface, it is quite prominent at the top of Facha Unit (figure-5 & figure-6). Northward the structure is bounded by a low semi closure (graben shape) labelled L1 with an estimated area ~330km^2. Due to the limitation of the data coverage the west boundary of this graben is undefined, two fault zones are

Licensed Under Creative Commons Attribution CC BY

formed the graben, first one is the fault zone-3 at the south flank, which is consists of a group of parallel to sub-parallel normal faults dipping northward. The accumulation heave of this fault zone is ~1.0 km and the sum of the total throw is ~0.27 sec, the deepest unit affected by these faults is the pre-Upper Cretaceous unit (figure-6). The fault zone-3 obviously caused that the time-stratigraphic units younger than the Lower Eocene (upper blue interpreted surface) in the foot-wall to be thinner than the equivalent units in the hanging wall, which confirms that during the Mid-Eocene time these faults were active. Unlike the fault zone-1 were the fault's dips decreases with depth, the dip of faults in this fault zone is fixed. The second fault zone is fault zone-4, which has a maximum heave of (~600 m) and vertical motion (~523 m), the thickness of the hanging wall units is thicker than in the foot wall, but the deference is being less than had been observed in the previous fault zone. Units younger than the Lower Eocene characterized by the presence of the rollover anticline form along the main fault of this zone, this feature disappears with depth. Number of produced wells (P1-72, F3a-72, T1-72, and A1-NC73) were drilled at the flanks of the structure high-2 as shown in the figure (6).

The deepest interpreted horizon is the top of the acoustic basement, and due to the limitation of seismic data penetration, this basement may not consisted with the basement determined from gravity data. True basement (pre-Cambrian basement) mostly composed of intensively fractured and deeply weathered of Pan-African age granophyric granite, ranging between 670-460 Ma, (Williams, 1971 and 1972).

The producing of hydrocarbon from the basement rocks is known in some reservoirs in the eastern part of Sirt Basin. The time structure map of the top basement in the study area (Figure-7) confirm that the Barrut Arch (H1) in the north part is a basement-rooted structure that gently dipping eastward and steeply dipping northern and southern ward, the morphology of this surface underwent a large depression as a result of the impaction of the previous described fault zones. H3 is another high structure dominated the south part of the area (Figure-7), which also impacted by several NW-SE normal faults, and considered as the third prospect in the area.

The thickness variation of the deepest sediment succession is demonstrated by the isopach map of the pre-Upper Cretaceous unit (Figure-8) which shows the distribution of many closures with varies of low and highs peaks, caused by the impact of the unconformity surface that caps this interval of deposition (top basement- base of Upper Cretaceous), the map displays only the present day thickness which has a maximum value of ~2400 m at the south and decrease to the less than 300 m at the north east of the area center. It is noteworthy that the unconformity of the top surface of this package and the faulting impact are both controlled this variance of thickness. Tectonically this package of strata is controlled by the first rift phase which likely began older than Cretaceous and continued through the early Cretaceous time.

4. Tectonic Subsidence Analysis

Group of six wells (G1a-72, P1-72, F3a-72, T1-72, A1-NC177, B2-NC177,) located in the study area, in addition to three other wells (S1-72, Q1-72, and U1-72) located nearby to the south were used to study the tectonic history of the area, the analysis shows that the study area passed with four main tectonic stages, the first stage was the initial rift phase which started proximately at the Mid-Cretaceous time (~100Ma) during which the area underwent a significant amount of subsidence, the second stage began at the ~84 Ma (Campanian time) and characterized by a slow post-rift subsidence persisted until ~65 Ma, sequentially the initiation of the second rift phase took place, and a rapid syn-rift subsidence had been accrued and continued through the Paleocene–Eocene time producing a large amount of subsidence estimated by (400m – 615m).

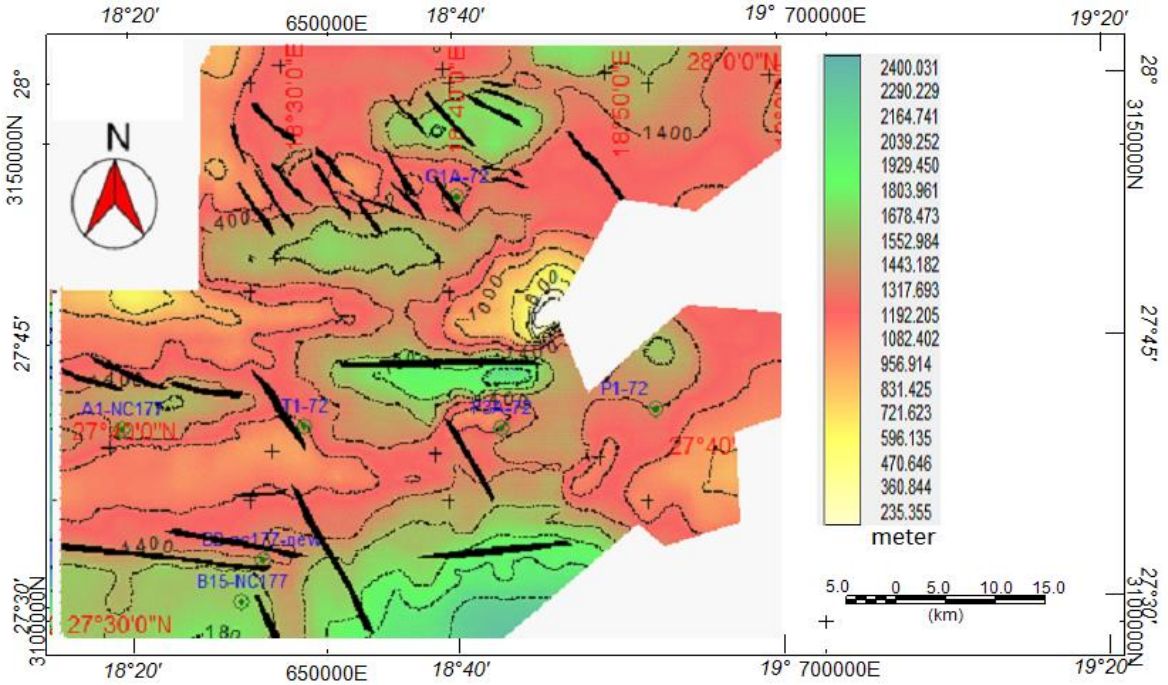

Figure 8: The isopach map of the Pre Upper Cretaceous succession, the map reveals the general southward increase of thickness, The contour interval is (200 m).

Licensed Under Creative Commons Attribution CC BY

At about 40 Ma (Bartonian time) the second post- rift subsidence was begun and still persisted to the present day (figure 9).

The tectonic subsidence curves (TS) for the previously mentioned wells which produced by creating a back-stripping for some depositional units are shown in (figure-10), it is noteworthy that this recovered (TS) were computed without applying any sea-level or paleo-bathymetry corrections. The TS curves for the all available wells show the first phase of the subsidence (initial rifting phase) which took place during the Late Cretaceous 'Cenomanian through Santonian' (100 Ma – 83.5 Ma), with a maximum of 630m at well A1-NC177 and a minimum of 121m at well B2-NC177. Subsequently, this initial rifting phase was followed by a slower period persisted until 65.5 Ma (Campanian and Maastrichtian), probably refer to the thermal subsidence period. Johnson and Nicoud (1996) termed this stage by the *rift-infill phase*. The TS curves show also a second rapid subsidence phase, identified hear as a second rift phase, during the period of Paleocene - Mid-Eocene, that corresponding to the fault-activity phase in the late Paleocene-early Eocene (Gumati et al., 1991). Ultimately, the last stage of the subsidence appears on all the tectonic subsidence curves for the used wells as a slower subsidence episode, which considered as the second thermal subsidence phase started in the late Eocene ~40.4 Ma and persisted to the present day. The subsidence range during this phase is about 17 m at well S1-72, and 121 m at well G1a-72, as minimum and maximum values respectively.

4.1 Estimation of the stretching factor (β) value

It is known that there are varies method to calculate the stretching factor (β) value. in this study, the using of the computed tectonic subsidence curves was the approach, by which we looking for the best matching between the observed and the calculated curves through the program (Basin Analysis Toolbox program), the theoretical tectonic subsidence curves created based on the McKenzie's (1978) equations. The derived curves from the 9 actual wells have been fitted to those theoretical curves, figure-11 shows the best fit has been obtained for each single well.

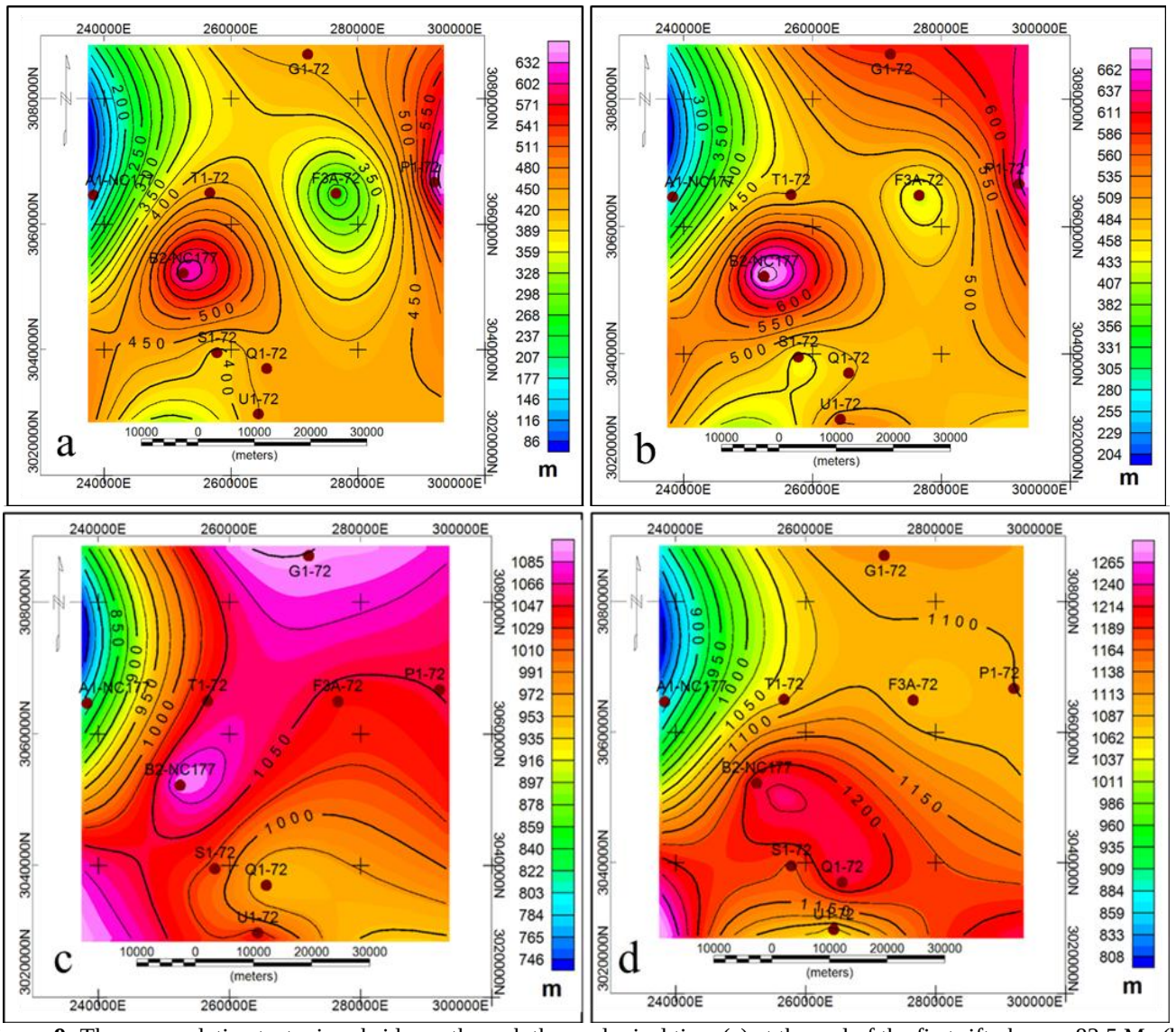

Figure 9: The accumulative tectonic subsidence through the geological time (a) at the end of the first rift phase ~ 83.5 Ma (b) at the end of the first thermal basin sagging ~65.5 Ma, (c) at the end of the second rift phase ~48.3 Ma, and (d) the present day

Licensed Under Creative Commons Attribution CC BY

It is worthy to clarify that the used program for this purpose has an optional setting for one rift phase or two rift phases for more suitable comparison. We applied the second option, since the characters of the observed curves are strongly suggests that there are two rift phases. The displaying of the results for the two rift phases reveals multi stretching values distributed through the area. During the first rift phase, the range of β values are 1.045 - 1.14, from which the maximum crustal stretching value has been estimated and found about 14%, this maximum value recorded at well B2-NC177. During the second rift phase the range of β values are 1.07 and 1.12, this indicating that the maximum value of the crustal stretching was 12% recorded at the wells S1-72 and Q1-72. However to obtain the net value of the total tectonic subsidence from both rift phases, we calculated the product of the multiplies of the both values (first and second β values) for each single well, the final result shows that the minimum and maximum β values in the study area are 1.157 and 1.226, these values pointed that the maximum stretching of the crust was 22.6%, obtained at well B2-NC177.

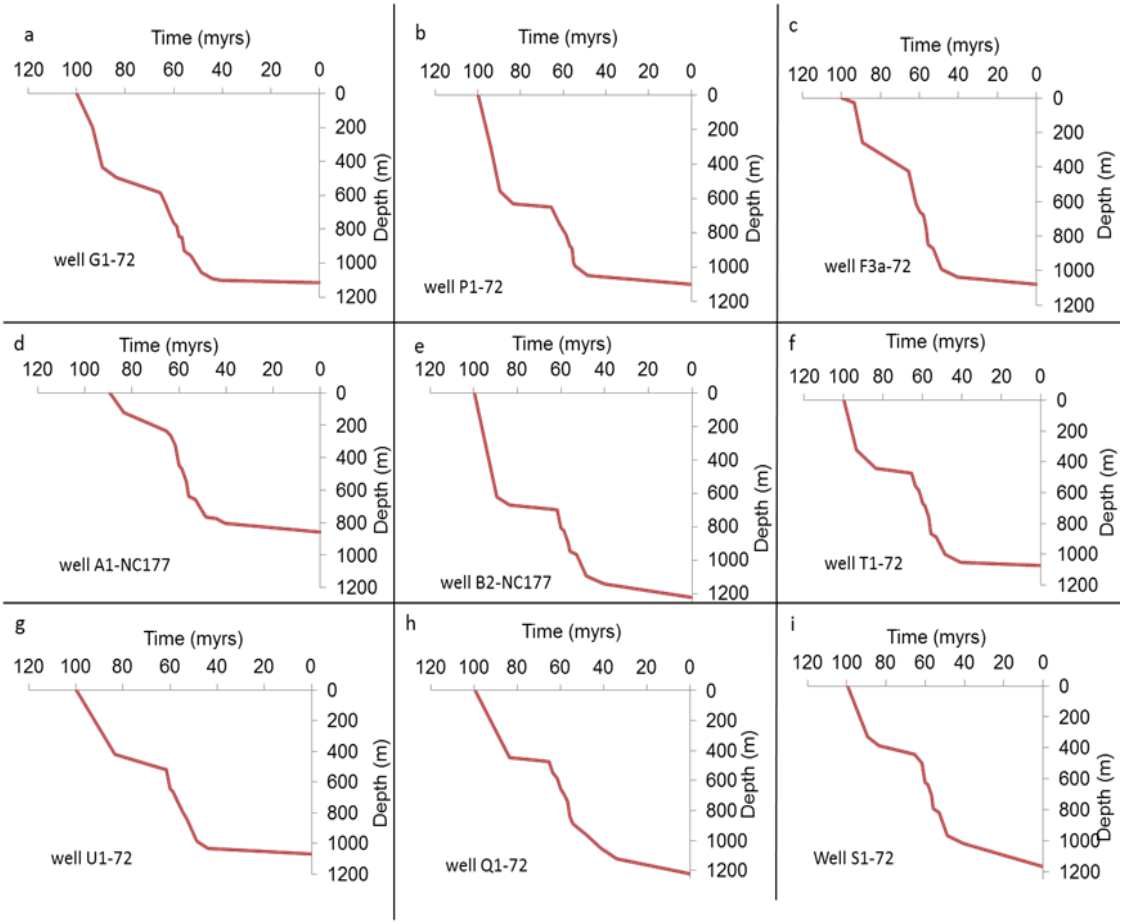

Figure 10: The tectonic subsidence curves, evaluated from the stratigraphic data of 6 boreholes distributed in the study area and 3 others close to the south (see the previous figures for the location). All the curves of used wells show the common shape of a normal extension basin, with alternative phases of rifting and thermal sagging

4.2 Comparisons with previous published tectonic studies

The availability of well data in the Sirt Basin encourage many researchers to study its subsidence history, i.e. Gumati et al. (1991), Van der Meer and Cloetingh, (1993a), Tmalla 1996), Abadi et al (2008). Two previous studies have been chosen for the result comparison, (Gumati et al., 1991), 'further will be noted as S-1', and (Abadi et al., 2008), 'further will be noted as S-2'. Both studies (S-1 and S-2) were a regional studies.

The comparison will be restricted to the results related to area of my study. The subsidence results of well G1a-72 have been used for Comparisons with S-2 (figure-12, a & b), some maps of the accumulative tectonic subsidence have been used from S-1 (figure 12, c and d). In general, both studies suggested that there were multi mutual rapid rifts and thermal sagging phases. Gumati and Nairn (1991) demonstrated four main phases, similar to what have been obtained from this study. Abadi et al. (2008) subdivided the main phases into relatively short sub-phases based on each single change in the rate of tectonic subsidence. The TS curves of the common well G1a-72 for S-1 study, and this study have quite similar shape but slightly differ in the accumulatively amount of the tectonic subsidence versus time (probably due to the different used programs). The three studies show the magnitudes of the accumulated TS for the initial rift phase (~90 Ma) as following: S-1 at this age the result not shown, S-2 is ~390 m, and this study is ~432 m. regarding the second stage which is denoted in this study by the 'first thermal sagging

Licensed Under Creative Commons Attribution CC BY

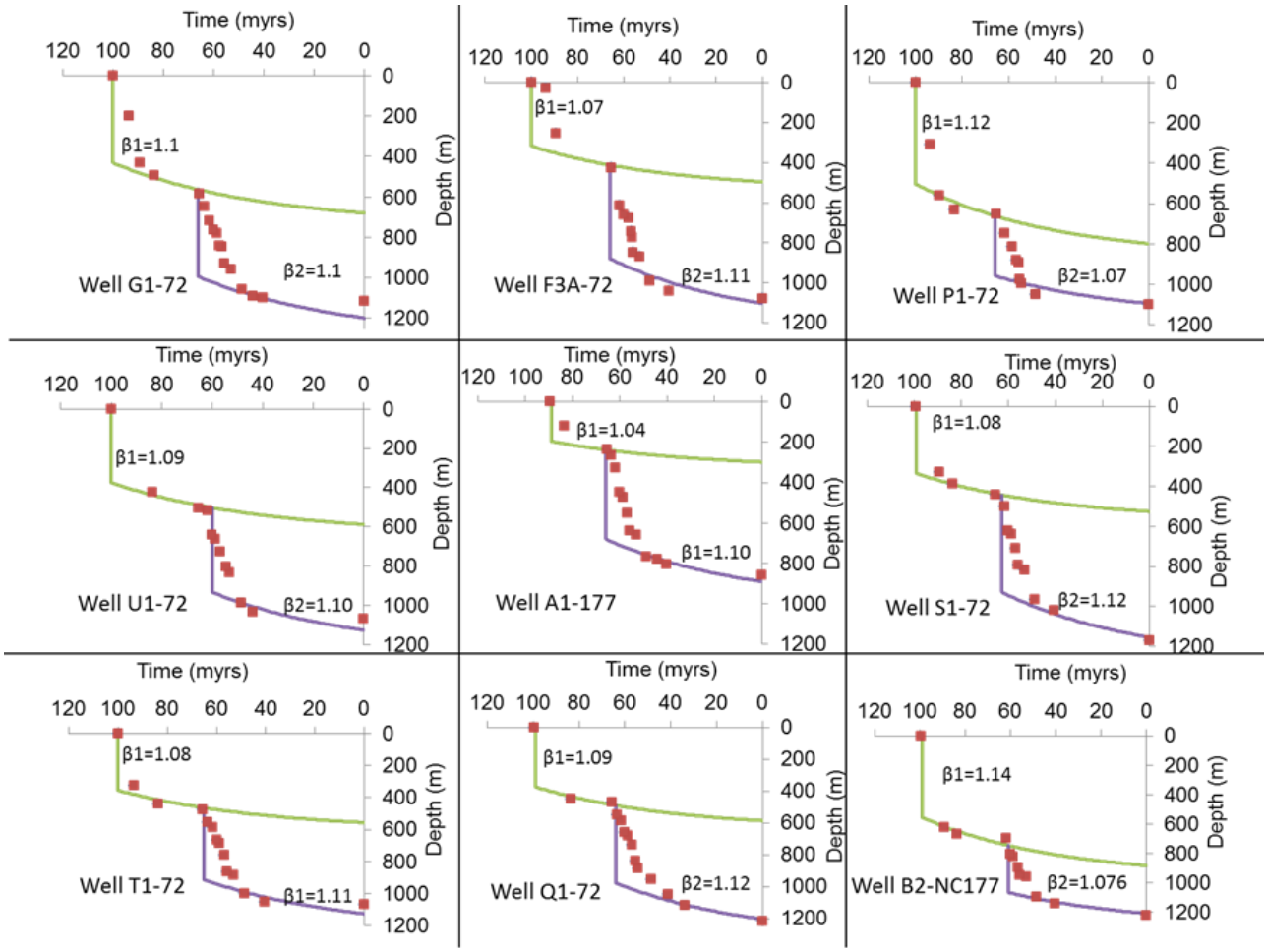

Figure 11: Estimation of (β) values, by obtained the best fit between the computed Tectonic subsidence curves of the nine wells with the expected subsidence Theoretical curves which based on the McKenzie's (1978) equation

phase (~65 Ma), the accumulative TS obtained by the study S-1 is about 600 m, and by the study S-2 is about 530 m while by this study S-3 is about 586 m. By nearly the end of the second rapid rift phase (~50 Ma) the accumulative TS values obtained from the three studies S-1, S-2, and S-3 are 1400 m, 735 m, and 1056 m respectively. Ultimately the final maximum accumulation of TS at the present time from S-2 and S-3 are 830 m, and 1116 m respectively, and unfortunately S-1 does not show the value for this interval.

Table summarizes these tectonic subsidence values versus time from the three studies.

Table 1: Summarising the tectonic subsidence values in meters at the point location of well G1-72 as computed from three different studies (Saleem, 2015)

Age (Ma)	*Gumati study (S-1)*	*Abadi study (S-2)*	*This study (S-3)*
90	Not shown	390	432
65	~600	530	586
50	~1400	735	1056
present	Not shown	830	1116

4.3 The impact of paleo-water depth in the subsidence calculation

It is obviously that the sediments load and the thermal contraction are the main factors that have the strong impact on the basins rift (Watts et al., 1984).however, additional to that there are a group of other factors when they combined together they have significant roles on the final result of the basin rift, such of these are; paleo-bathymetry, global sea-level changes, unconformities, and climate evolution & erosion. The missing of any published quantitative data regarding the paleo-water depth in the study area may be that made the estimated values of the paleo- bathymetry are not highly dependable.

Licensed Under Creative Commons Attribution CC BY

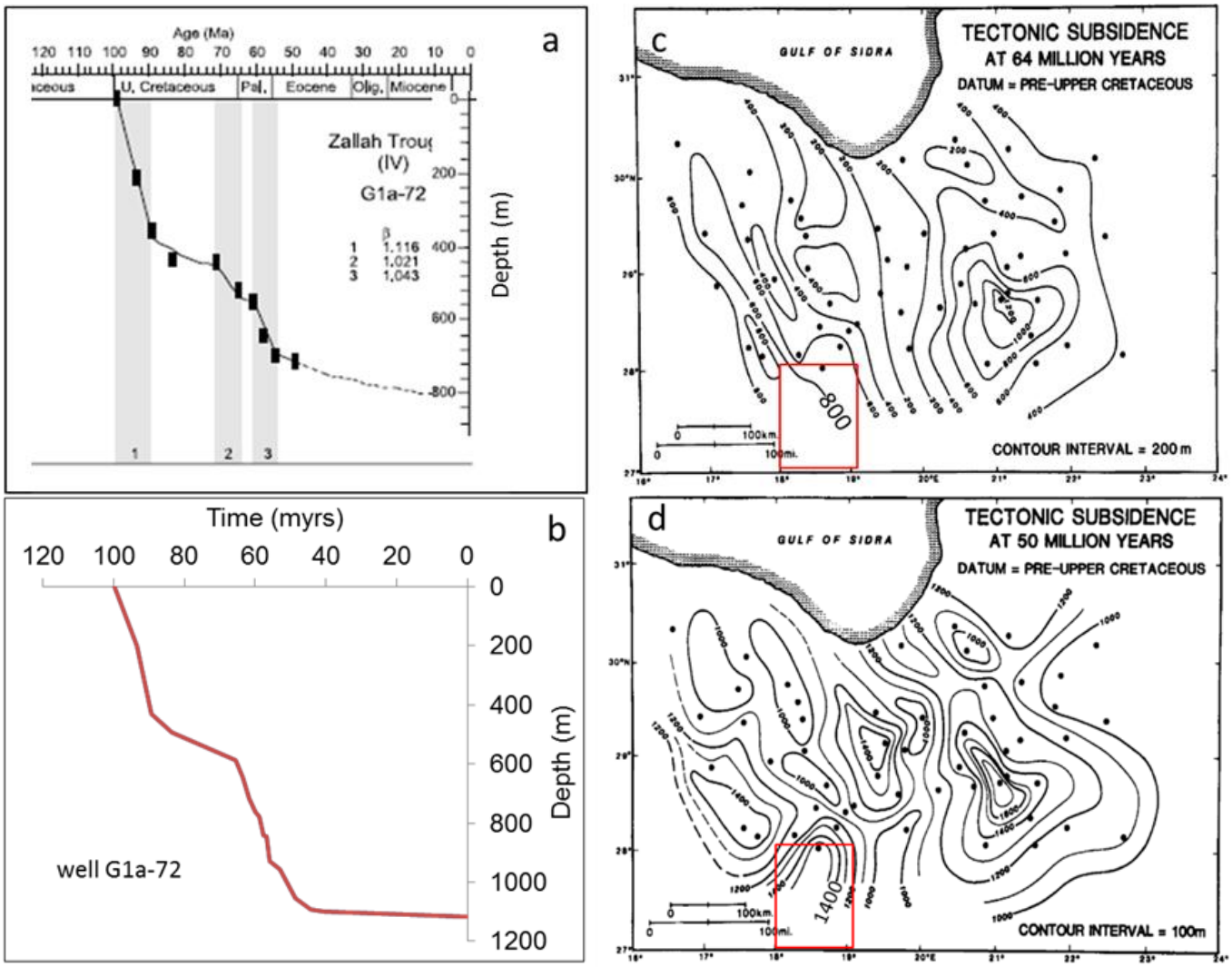

Figure 12: (a) and (b) The calculated tectonic subsidence curve (TS) at the well G1a-72, estimated by the study of Abadi et al (2008), and by this study respectively. (c) and (d) show the maps published by Gumati et al. (1991) for the accumulation of the tectonic subsidence of the Sirt Basin at 64 Ma and at 50 Ma respectively,. The red bounded area define the location of this study

Therefore to make sure that the estimated values are as close as possible to the reality, all the available information related to the sedimentary units and their depositional environments have been gathered, as well as the confirmed information about the fossils that found within each single sedimentary unit of the stratigraphic column of the area.

Based on the collected information, and with help of one of the expertise (pers. Comm., 2014), the paleo-bathymetric values for each sedimentary units have been estimated. All the estimated values is restricted by the information identified by Bezan (1996) and Muftah (1996), which documented that the depth of the paleo-water in the Sirt Basin never exceed 200 m. The estimated paleo-water depth for each sedimentary unit is shown in table-2, where slightly changed in some wells according to the somewhat variation in the relative percentages of lithology identified in these wells. Ultimately the paleo-water depth values have been used to produce the new tectonic subsidence curves (TS) as shown in figure 13. To give a clear comparison, we plot three different application simultaneously for every single well, the first (blue), resulted from no paleo-water depth applying (zero paleo-water depth), the second (brown) and the third (green) resulted from applying the minimum and maximum paleo-water depth respectively. One can note, that the general shape of the curves is more or less the same (blue and brown) while applying the minimum estimated values (0-45 m), However when the maximum estimated values are applied (40 m-200 m), an obvious drop down in the curves is resulting, which reflect the increase in the subsidence value.

Licensed Under Creative Commons Attribution CC BY

Table 2: The minimum and maximum paleo-water depth values that assigned for different stratigraphic units which used to produce the new tectonic subsidence curves, after (Saleem, 2015)

Unit name	*Age*	*Ma*	*Max dept. (m)*	*Min. dept. (m)*
Augila	U. Eocene	0-40	40	10
Gialo	Mid Eocene (Lutetian)	40.4-48.6	120	30
Gir	L. Eocene(Ypresian)	48.6-53	80	20
Facha	L. Eocene	53-55.8	130	30
Zeltan	U. Paleocene (Thanetian)	55.8-56.8	180	45
Dahra	Mid Paleocene (Selandian)	56.8-61.7	130	25
Beda	L. Paleocene (Danian)	61.7-63.5	70	15
Hagfa	L. Paleocene (Danian)	61.7-65.5	180	45
kalash	U. Cret (Maastrichtian)	65.5-83.5	100	25
Rachmat	U. Cret. (Santonian)	83.5-89.3	200	45
Etel	U. Cret. (Turonian)	89.3-93.5	100	25
Early U. Cret	U. Cret (Cenomanian)	93.5-99.6	120	35

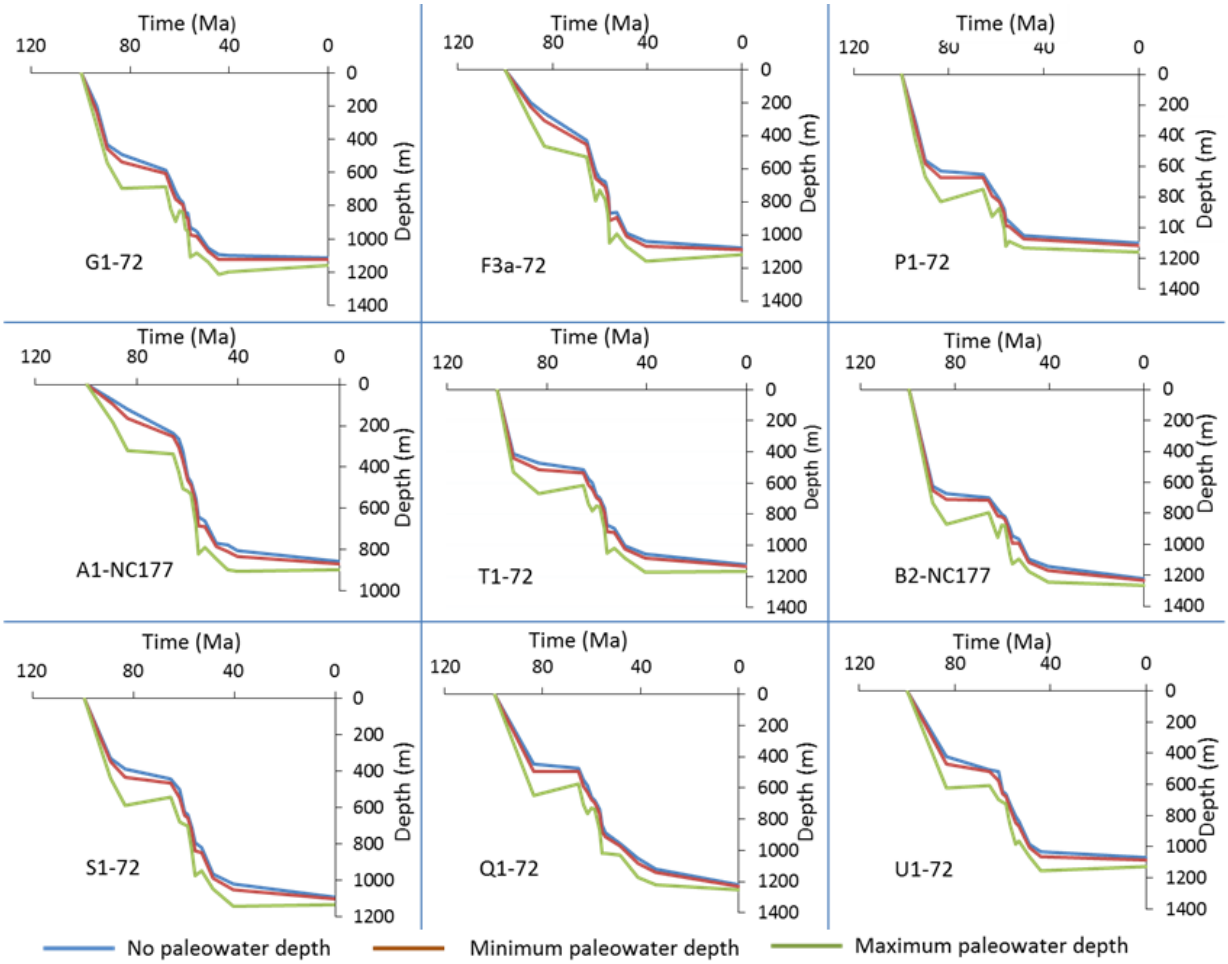

Figure 13: The impact of applying the paleo-water depth on the subsidence curves of the used wells.
Note: that the same previous stratigraphic information from the 9 boreholes has been used

4.4 The effect of the global sea level change on the tectonic subsidence

The determination of the amount of eustatic variations along the depositional geological time is not easy task (Guidish et al., 1985; Burton et al, 1987; Kendall and Lerche, 1988), and due of that, the different long-term sea-level change that have been estimated by a number of authors, revealed significant variation, especially at the Late Cretaceous time (Miller et al., 2005). To clarify this variation we can see some examples of the previous attempts of estimating the global sea-level changes such as; Vail et al. (1977) who consider the depositional sequences as a base of his own Estimation (Mitchum et al., 1977); Pitman (1978) follow a different method in which he has suggested that the long-term fluctuation in the sea level scale can be result only by the change in the length and rate of the seafloor spreading. While Watts & Steckler (1979), based their estimation on the paleo-environmental and the stratigraphic record data. The more recent curves have been published by Miller et al. (2005), which is similar to what proposed by Watts and Steckler, put it is less in the magnitude, the mentioned curves are shown in (

Licensed Under Creative Commons Attribution CC BY

Figure). The curves of Watts & Steckler (1979) and Miller et al. (2005) have been used to observe the impact of the global sea-level change during the geological time in the study area, as shown in

Table, by applying these values for the 9 used wells A new tectonic subsidence curves were produced as shown in (Figure). It is clear from the produced curves that at all the wells, the application of (Watts and Miller) values of sea-level change always cause a slightly reduction to TS depth, however the reduction of Miller Model is little bit less than the one by Watts.

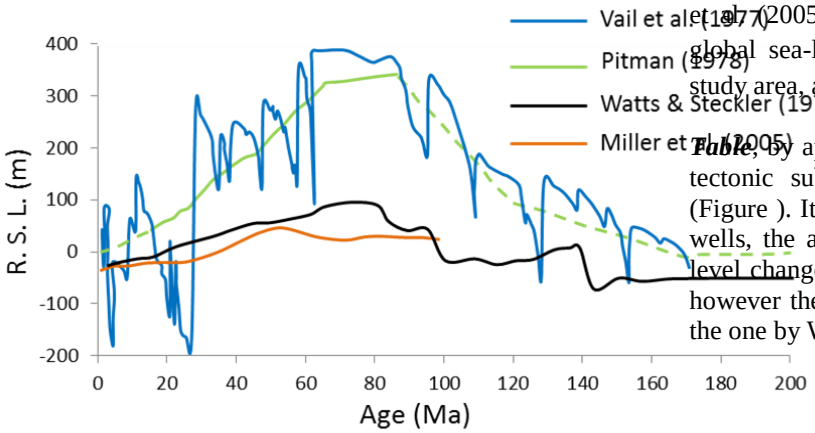

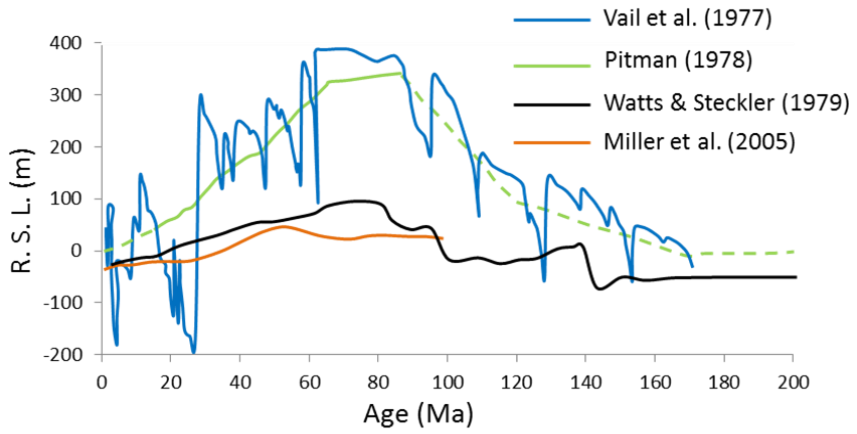

Figure 14: The Global relative sea-level change, as estimated by Miller et al. (2005) (brown line); Watts & Steckler (1979) (black line); Pitman (1978) (green line); and Vail et al. (1977) (blue line). Modified from Watts et al. (1984).

Table 3: Sea level change versus time (Ma), relative to the present day sea-level, constructed from the published curves of Miller et al. (2005) and Watts et al. (1979)

Age (Ma)													
0	33.9	40.4	44.3	48.4	53.5	55.8	57.7	60	65.5	83.5	90	93	99.6
Watts Model (m)													
0	48	60	65	75	75	80	80	85	100	75	60	58	10
Miller Model (m)													
0	20	35	50	58	60	59	52	50	42	45	44	42	40

Licensed Under Creative Commons Attribution CC BY

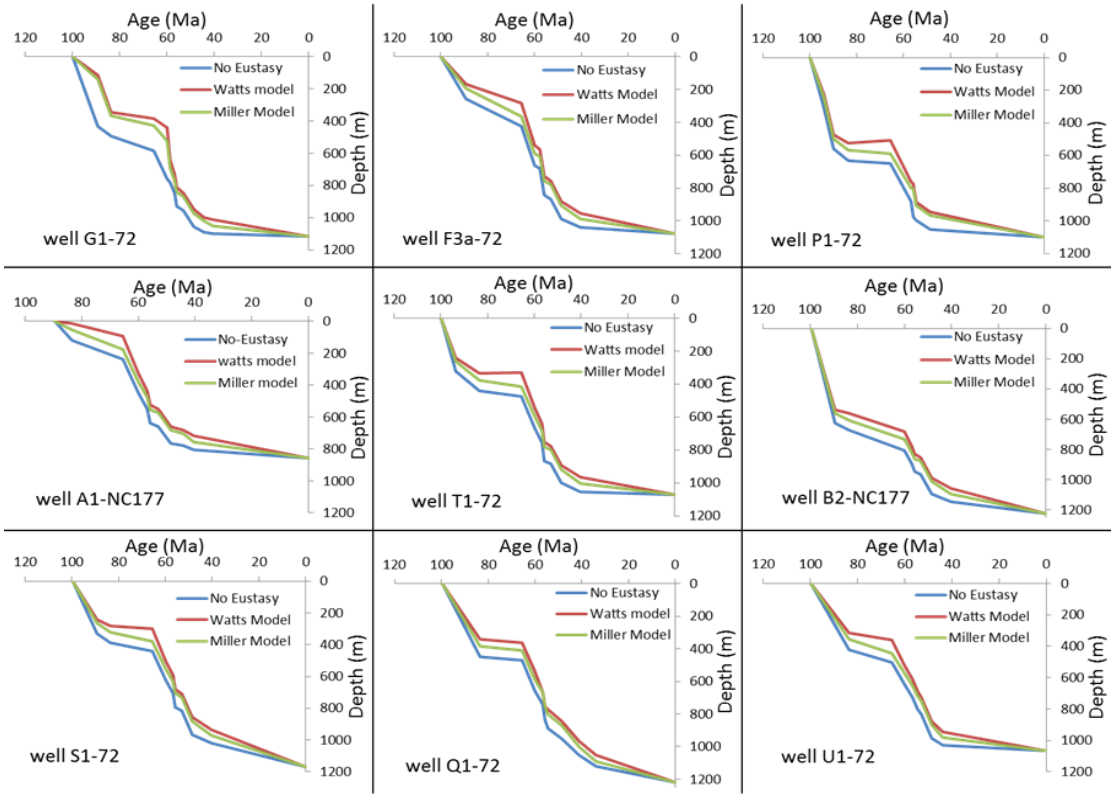

Figure 15: The impression of the sea-level change, onto the tectonic subsidence curves of the available nine wells in the area of study. The effect is negligible at most of the wells, and just a small change in the curves shape occurred

5. 2D Gravity Modelling

To add more valuable analysis to the current study, two gravity models have been constructed along two profiles A-A1 and B-B1 by utilizing the modeling facility (GM-sys) program. The density values for the modeled units were obtained from the density logs of the available wells, or from the composite information of the units (lithology and porosity). The estimated density values of the unities are shown in (table- 4). The boreholes information and the interpreted seismic sections were used as a control tools for the gravity models. The strike direction of each profile has been chosen to pass through the good coverage areas and to cross cut the dominant anomalies (figure-16).

5.1 Model A-A1

The first E-W profile A-A1 is proposed to simulate the subsurface units until the basement depth, and to approach this target we used the residual gravity anomaly after removing the regional filed from the Bouguer anomaly. Figure- 17 demonstrates the final shape of the A-A1, the profile is 108 km long. The model attempted to simulate the same depositional units as having shown previously on the interpreted seismic data of the area of study.

As one can note, that the model suggests an average depth for the top surface of the basement ~ 5.25km (minimum 4.6km and maximum 5.7km). The consistency of the basement depth that obtained from the gravity model and the one obtained from the seismic data is not always satisfying, this variation in the depth values occasionally result from the miss define the right horizon that represents the true basement due the low resolution of the seismic data, or from the other hand could be as a result of the miss-define the proper density of the model units. The model reveals a structural high (an anticline) at the middle of the profile where affected by a number of major faults, that possibly being the reason for increasing the hydrocarbon potentiality of this structure since a number of produced wells were drilled. A group of other faults were noted to the right and left of this high structure. Most of these faults dipping eastward with angles range from 50 -60 degrees, others are dipping westward. One can note that all the faults are nearly parallel normal faults which may confirm that they are most likely related to the same tectonic event (extension event).

Licensed Under Creative Commons Attribution CC BY

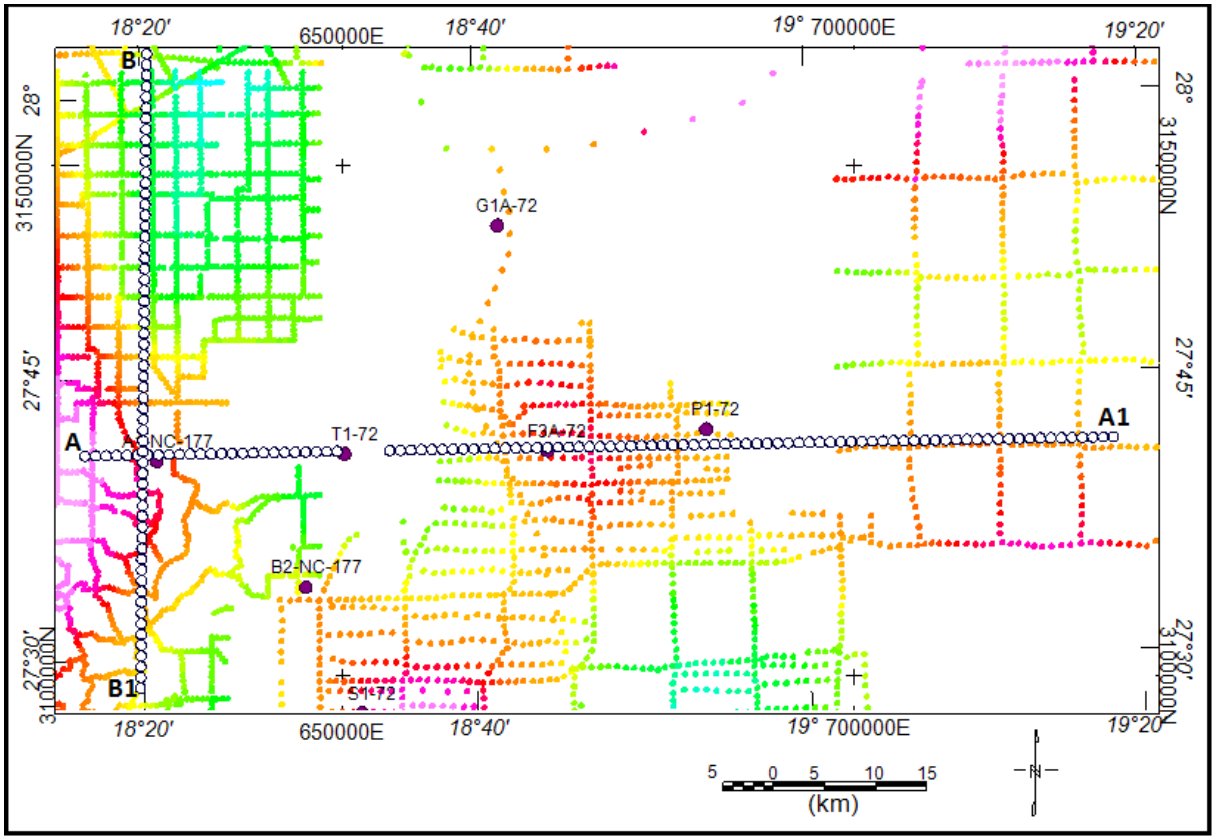

Figure 16: Showing the gravity data coverage and the location of the profiles A-A1 and B-B1

Table 4: The assigned densities for the different Units estimated from a group of wells in the area of study, after Saleem (2015)

Unit name	S. U.	Gialo (M. Eoc.)	Gir (L. Eoc. 2)	Facha (L. Eoc.1)	Beda (Paleoc.)
Density g/cc	1.938	2.198	2.5	2.485	2.559
Unit name	U. Cret.	Pre- U. Cret.	Basement	L. Crust	Mantle
Density g/cc	2.597	2.621	2.67	2.75	3.3

5.2 Model B-B1

The second model has been constructed along the N-S profile B-B1 with a length of 62.5 km. The simulated depositional units have been given the same density values as in the model A-A1. In this model, the deep crust layers until the Moho depth were targeted for simulation. The upper part of the model is zoomed in (Figure-18) from which it is noticed that another structural high exists at km 42.5 from the north begging, the high seems to be a produced trap where some oil wells were drilled such as A1-NC177, the minimum and maximum depth of the top surface of the basement are 4300m and 7290m respectively. The lower part of the simulated model is shown in (figure-19) which demonstrate the morphology of the basement, lower-crust, and Moho surfaces, the minimum and maximum depth of the Moho are 27600m and 33450m respectively. These four depth values for the basement and Moho will give us an indication of the crustal extension factor (β). According to the McKenzie (1978), McKenzie (1985), and McKenzie (1988) the variation of the Moho and basement depth can gives an estimation of the crust extension factor (β), since β=L/L1 where L is the original thickness of the crust (29.15km), and L1 is the thickness of the thinned crust (20.31 km). Therefore, the estimated value of the β factor in the study area regarding to this model is ~1.43.

Licensed Under Creative Commons Attribution CC BY

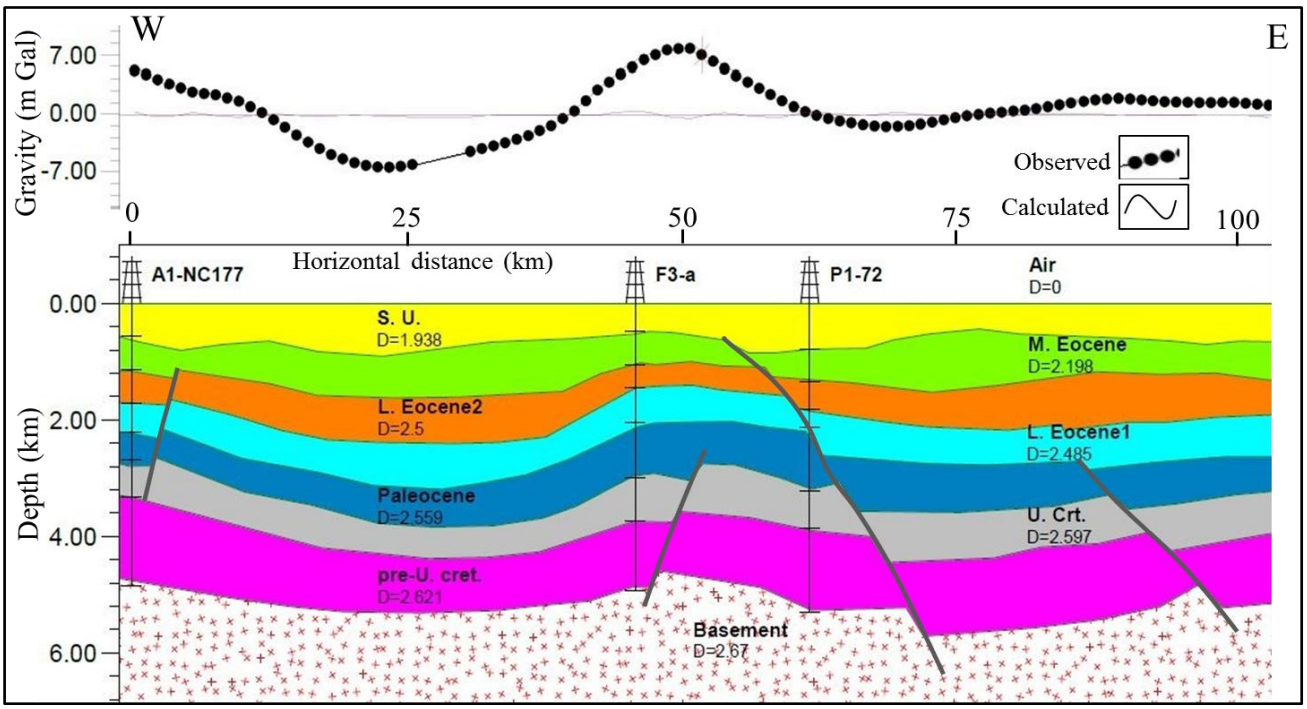

Figure 17: The upper part of the model constructed from the W-E profile A-A1, the model reveal the The structural high at the midel of the profile and number of faults afected the area

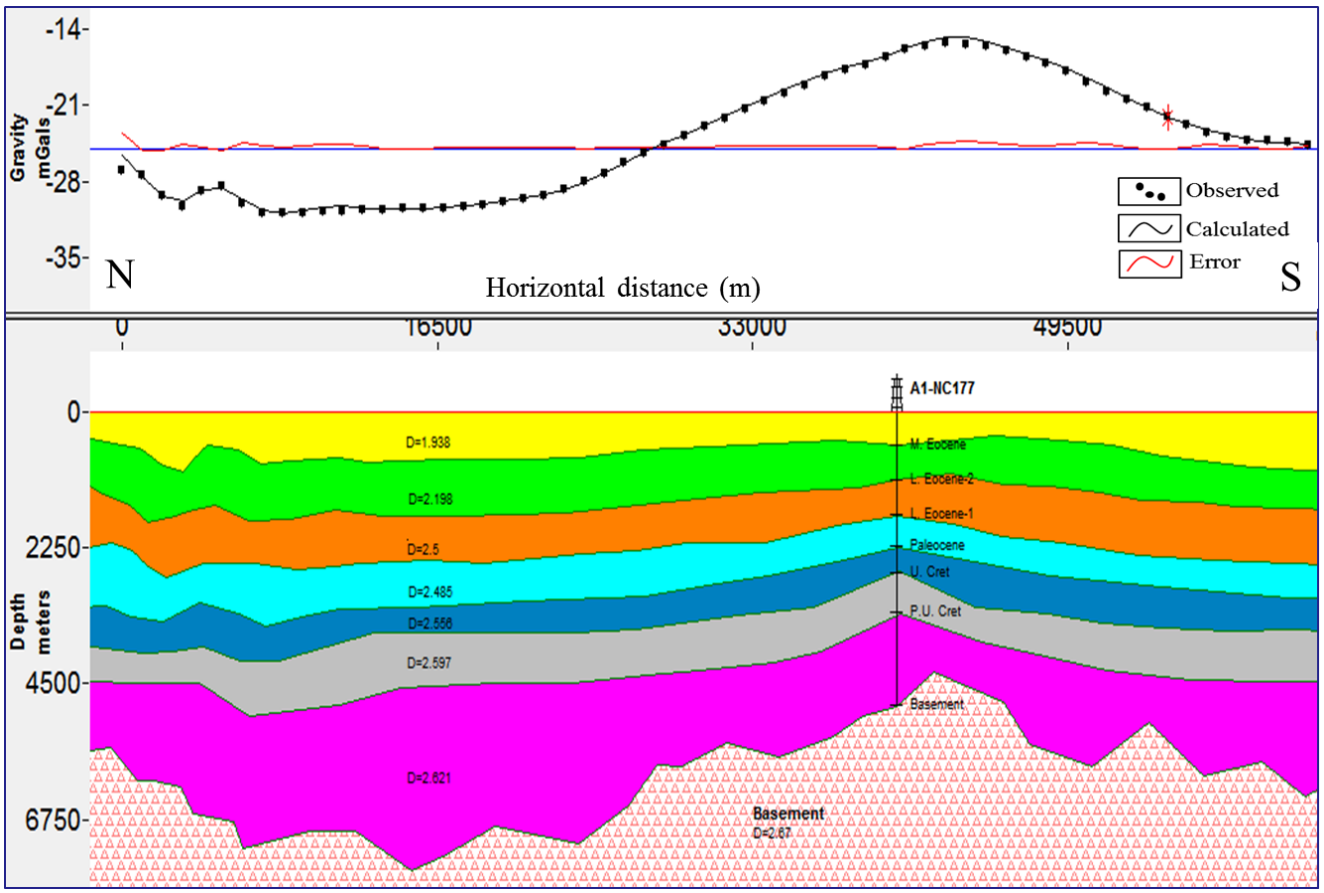

Figure 18: The upper part of the model constructed from the N-S profile B-B1, the model reveals the deep seated structural high

Licensed Under Creative Commons Attribution CC BY

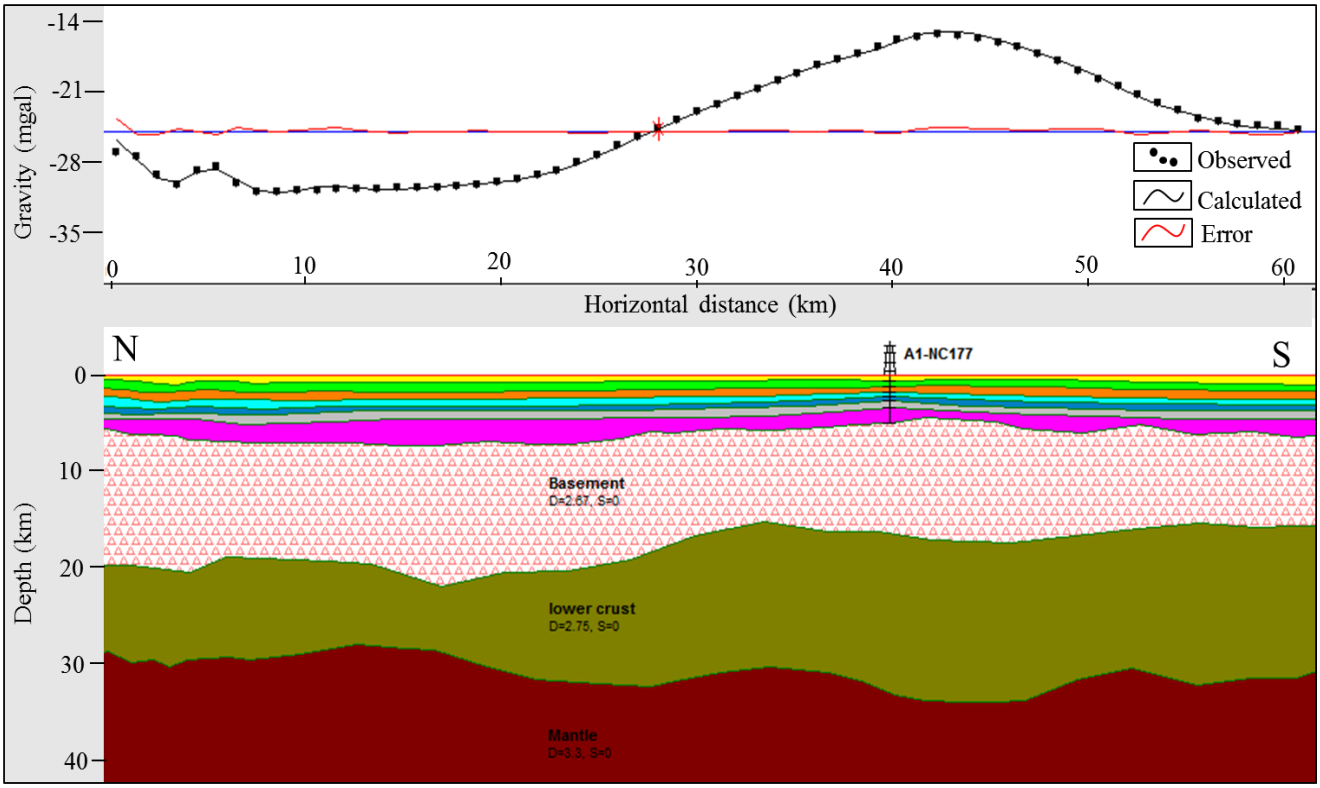

Figure 19: Regional gravity model B-B1 zooming the lower crust surfaces till the Moho interface, from which the minimum and maximum crust thickness has been estimated and further the stretching factor was calculated

6. Results, Discussion, and Conclusion

Seven seismic horizons trough the 2D and 3D seismic data that covering the area of study, representing multi important surfaces and marks in the area were interpreted, the interpretation revealed that a number of fault zones are dominated the area of study. These fault-zones impacted the strata units and controlled their thickness. It is suggested that they are either young faults or may be resulted due reactivation of older basement structures, because it is observed that most of these faults are cut the Cenozoic deposition (late post-rift) and show respectable changes in thickness during the post-Eocene. These fault zones are:

Fault zone-1, in the north part of the area, caused a total heave and throw of ~1.0 km and ~0.3 sec respectively. With a ramp master fault propagating deeply along the strata, these faults are younger than the Mid-Eocene, since they crosscut the formation of this age (Gialo Formation) and the older units below; the faults can be traced as deep as the Upper Cretaceous, and have significant impact on the Barrut Arch structural high.

Fault zone-2, has a maximum throw of 0.058 sec (~162 m), its age is also younger than the Mid-Eocene, and propagate deep to the top of Upper Cretaceous, from which it believed that they are related to the post-time of the second rift phase (Upper Cretaceous - Mid-Eocene).

Fault zone-3 forming and define the south flank of the structure low L-1 which has the graben shape within the Enaga-4 area, group of parallel to sub-parallel normal faults performing this fault zone with a northward dipping direction, the net sum of heave and throw is ~1.0 km and ~0.27 sec respectively, most of these faults are post Mid-Eocene in age, but they extended deeply to the pre-Upper Cretaceous unit. Obviously, the fault zone-3 caused that the hanging wall time-stratigraphic units being thicker than their equivalent units in the footwall, since in some area, such as the graben L-1the maximum variation in thickness exceeds 300 m.

Fault zone-4 define the north flank of the graben L-1, it caused a maximum heave of (~600 m) and throw of ~0.16 sec (~523 m) the throw is being decreases with depth. Comparing with the fault zone-3 the deference in thickness of the stratigraphic units in the hanging wall and foot wall is less. Along the main fault of this zone the most upper layers (above the top of Lower Eocene) distinctly have a rollover anticline shape appearance, and this phenomenon disappears as we move deeper.

The majority of faults in the study area extending NW-SE (N31˚-60˚W), some are E-W trending, and others, essentially under the top of Cretaceous, are NE-SW. the interpretation shows that the Barrut Arch in the north part of the area is a deep-seated (basement rooted) structural high, which is sectioned due to the fault zones into two parts. The NE part performs a rollover anticline in the hanging wall of fault zone-1, while the SW segment performs the footwall of Fault zone-1, the arch is also predominated by a group of parallel faults performing the fault zone-2. The interpretation reveals that the footwall of the fault zone-3 which located in the area of Enaga-4 represents another structural high (H2),

Licensed Under Creative Commons Attribution CC BY

this structure formed a significant trap for the hydrocarbon of the Facha Unit (one of the produced units in the area). The structure extends in depth from lower Eocene unit until the pre-Upper Cretaceous unit where it becomes gentler.

In addition to these structural-highs there are number of grabens distributed in the area adjacent to these highs, with different geometries and depth, as following:

Graben shape structural low (L1) which is a semi-closure included within the Enaga-4 area, the graben being bounded southward by the fault zone-3 and northward by fault zone-4.

Low structural (L2), adjacent to the Barrut arch from the northwest side, is expected to be an extension of structure (L1), but the lack of data does not allow us to confirm this explanation.

Structural low (L3) included within the Enaga-3 region, has E-W elongated shape, bounded from the south by a highly faulted area.

the basement depth map and the pre-Upper Cretaceous unit thickness map both are exceedingly demonstrate the Abu Tumayam deep Trough, but the overlying stratigraphic units show an inverse dipping of their strata (northward dipping) due to the big unconformity took place after the end of the pre-upper Cretaceous caused the trough area appears as an elevated area on the younger units maps.

Obvious there are four noticeable events in the tectonic subsidence values due the applying the high values of the paleo-water depth. First of them is nearly at the end of the first rift phase (~83.5 Ma), resulted when we applied a value of ~200 m of paleo-water depth, this application made a reverse pattern on the second tectonic phase (first post rift phase) in most curves of the wells, that appear a slightly uplifted instead of getting subsidence.

The second and third noticeable events are during the time ~61.7 Ma and ~55.8 Ma (second rift phase interval), here the subsidence curves didn't go smoot but they show some troughs and peaks during its slope, due to the extremely relative changes in the values of water depth (80 m-180 m). The fourth event noticed about the subsidence curve of the last phase (second post rift, ~40.4 Ma) when 120 m water depth applied, this application also leads to a partially uplift in some wells since that time to the present.

7. Future Scope

The study has been performed on a limited area due to the limited data therefore the results restricted to this area. We attempt to continue the study to cover the entire basin with a borehole data for a significant number of wells and good coverage of seismic data. At the same time we can use other software such as the Move™ software for more investigation and extra quantitative information about the tectonic events that took place through the geological time.

References

[1] Abadi, A.M., Van Wees, J.D., Van Dijk, P.M., and Cloetingh, S.A.P.L. (2008) Tectonics and subsidence evolution of the Sirt Basin, Libya. **AAPG** Bull., vol. 92 (8): p. 993–1027.
[2] Anketell, J.M. (1996) Structural history of the Sirt Basin and its relationship to the Sabratah Basin and Cyrenaica Platform, northern Libya. First Symposium on the Sedimentary Basins of Libya, Geology of the Sirt Basin, vol. 3. (eds.) M.J. Salem, M.T. Busrewil, A.A. Misallati, and M.A. Sola, **Elsevier**, Amsterdam, p. 57-89.
[3] Baird, D.W., Aburawi, R.M. and Bailey, N.J.L. (1996) Geohistory and petroleum in the central Sirt Basin. First Symposium on the Sedimentary Basins of Libya, Geology of the Sirt Basin, vol. 3. (eds.) M.J. Salem, M.T. Busrewil, A.A. Misallati and M.J. Sola, **Elsevier**, Amsterdam, p. 3-56.
[4] Barr, F.T. and Walker, B.R. (1973) Late Ternary channel system in northern Libya and its implication on Mediterranean sea level changes. In: Initial Report Deep Sea Drilling Project, Leg 13. (Eds.) W.B.F. Ryan and K.J. Hsu, p. 1244-1251.
[5] Barr, F.T. and Weegar, A.A. (1972) Stratigraphic nomenclature of the Sirt Basin, Libya. **Petroleum Exploration Society of Libya**, Tripoli, 179p.
[6] Bezan, A.M., Belhaj, F., and Hammuda, K. (1996) The Beda Formation in Sirt Basin. First Symposium on the Sedimentary Basins of Libya, Geology of the Sirt Basin, vol. 2. (eds.) M.J. Salem, A.S. El-Hawat and A.M. Sbeta), **Elsevier**, Amsterdam, p. 135-152.
[7] Boote, D.R.D., Clark-Lowes, D.D., and Traut, M.W. (1998). Palaeozoic petroleum systems of North Africa. In: Petroleum. Geology of North Africa, (eds.) D.S. Macgregor, R.T.J. Moody, D.D. Clark-Lowes, **Geol. Soc**. Special Publication No. 132, p. 7-68.
[8] Burton, R., Kendall, C.G., and Lerche I. (1987) Out of our depth: On the impossibility of fathoming eustasy from the stratigraphic record, **Earth Sci. Rev**., 24: 237-277.
[9] DE Wit, M., Jeffery, M., Bergh, H. and Nicolaysen, L. (1988) Geological map of sectors of Gondwana reconstructed to their dispositions 150 Ma. University of Witwatersrand. Published by Amer. Assoc. **Pet. Geol**.
[10] Dercourt, J., Zonenhain, L.P., Ricou, L.E. et al. (1986) Geological evolution of the Tethys belt from the Atlantic to the Pamirs since the Lias. **Tectonophysics**, vol. 123: p. 241-315.
[11] Guidish, T. H., Kendall, C. G. S. C., Lerche, I. et al. (1985). Basin evaluation using burial history calculations: an overview. **AAPG** Bull., 69: p. 92-105.
[12] Guiraud, R. (1998) Mesozoic rifting and basin inversion along the northern African Tethyan margin: an overview. In: Petroleum Geology of North Africa, (ed.) D.S. Macgregor, R.T.J. Moody, D.D. Clark-Lowes, **Geol. Soc**. Special Publication No. 132,
[13] Gumati, Y.D., (1985) Crustal extension, subsidence, and thermal history of the Sirt Basin, Libya. **ESRI** Occasional publication No.3. Columbia, S. Carolina, 207p
[14] Gumati, Y.D., and Kanes, W.H. (1985) Early Tertiary subsidence and sedimentary facies, northern Sirt Basin, Libya. Bull. Amer. **Assoc. Pet. Geol**. vol. 69: p. 39-52.

Licensed Under Creative Commons Attribution CC BY

[15] Gumati, Y.D., and Nairn A.E. (1991) Tectonic subsidence of the Sirt Basin, Libya: **Journal of Petroleum Geology**, v. 14: p. 93–102.
[16] Hammuda, O.S., Sbeta, A.M., Mouzughi, A.J. et al. (1985) Stratigraphic nomenclature of the northwestern offshore of Libya. **Earth Sciences Society of Libya**. 166p.
[17] Johnson, B.A. and Nicoud, D.A. (1996) Integrated exploration for Beda Formation reservoirs in the southern Zallah Trough (west Sirt Basin, Libya). First Symposium on the Sedimentary Basins of Libya, Geology of the Sirt Basin, vol. 2. (eds.) M.J. Salem, A.S. El-Hawat and A.M. Sbeta, **Elsevier**, Amsterdam, p. 211-222.
[18] Kendall, C.G., and Lerche, I. (1988) The rise and fall of eustasy, in Wilgus, C.K., Hastings, B.S., Kendall, C.G.St.C., Posamentier, H.W., Ross, C.A., and Van Wagoner, J.C., (eds.) Sea-level Changes: an integrated approach: **Society of Economics palaeontologists and Mineralogists** special publication 42, p3-17.
[19] Klitzsch, E. (1971) The structural development of parts of north Africa since Cambrian time. First Symposium on the Geology of Libya (ed.) C. Gray. Faculty of Science, **University of Libya**, Tripoli, p. 253-262.
[20] Luning, S., Craig, J., Loydell, D.K. et al (2000a) Lowermost Silurian 'hot shales' in north Africa and Arabia: regional distribution and depositional model. **Earth Science Reviews**, vol. 49, p. 121-200.
[21] McKenzie, D., and Peate Bickle M.J. (1988) The volume and composition of melt generated by extension of the lithosphere, **J. Petrol**., vol. 29 (3), p. 625-679.
[22] McKenzie, D.P. (1978) Some remarks on the development of sedimentary basins: Earth and Planetary Science Letters, v. 40, p. 25–31.
[23] McKenzie, D.P. (1985) The extraction of magma from the crust and mantle: **Earth Planetary Science Letters**, v. 74, p. 81-91.
[24] Miller G., Michelle A. Kominz, et al (2005) The Phanerozoic Record of Global Sea-Level Change, **Kenneth Science** vol. 310 (25).
[25] Mitchum R.M.Jr., Vail P. R. and Thompson III S. (1977) Seismic stratigraphy and global changes of sea-level, part 2: the depositional sequence as a basic unit for stratigraphic analysis. In: C. E. Payton, Editor, Seismic Stratigraphy — Applications to Hydrocarbon Exploration, Memoir vol. 26, **American Association of Petroleum Geologists**, p. 53–62.
[26] Morgan, M.A., Grocott, J. and Moody, R.T.J. (1998) The structural evolution of the Zaghouan-Ressas structural belt, northern Tunisia. In: Petroleum Geology of North Africa, (ed.) D.S. Macgregor, R.T.J. Moody, D.D. Clark-Lowes, **Geol. Soc**. Special Publication No. 132, p. 405-422.
[27] Muftah, M.A. (1996) Agglutinated foraminifera from Danian sediment of northeastern Sirt Basin, in M.J. Salem, M.T. Busrewil, A.A. Misallati, and M.A. Sola, (eds.) The geology of the Sirt Basin: Amsterdam, **Elsevier**, v. 1, p. 233–242.
[28] Pitman, W.C. (1978) Relationship between eustasy and stratigraphic sequences of passive margins. **Geol. Soc**. Amer, Bull, 80, p. 1389-1403
[29] Ricou, L.E. (1994) Tethys reconstructed: plates, continental fragments and their boundaries since 260 Ma from central America to south-eastern Asia. **Geodinamica Acta**, vol. 7: p. 169-218.
[30] Tmalla, A.F.A. (1996) Late Maastrichtian and Paleocene planktonic foraminiferal biostratigraphy of well A1a-NC29A, northern Sirt Basin, Libya, in M. J. Salem, M. T. Busrewil, A. A. Misallati, and M.A. Sola (eds.) The geology of the Sirt Basin: Amsterdam, **Elsevier**, v. 1, p. 195–232.
[31] Vail, P.R., Mitchum, R.M. Jr., Todd, R.G. et al. (1977) Seismic stratigraphy and global changes of sea level. In Payton, C.E. (ed.) Seismic Stratigraphy– Applications to Hydrocarbon Exploration. **Am. Assoc. Petrol. Geol**. Mem., 26, p. 49–212.
[32] Van der Meer, F., and Cloetingh, S. (1993a) Late Cretaceous and Tertiary subsidence history of the Sirt Basin (Libya), an example of the use of backstripping analysis: ITC (**International Institute for Geo-information Science and Earth Observation**) Journal, v. 93(1) p. 68–76.
[33] Watts, A.B., and Steckler, M. S. (1979) Subsidence and eustasy at the continental margin of eastern North America, Maurice Ewing Symposium. Series 3, **AGU** Washington, D.C., p. 218-234
[34] Watts, A.B., and Thome, J. (1984) Tectonics, global changes in sea level and their relationship to stratigraphical sequences at the US Atlantic continental margin, Lamont-Doherty Geological Observatory and department of **geological Sciences of Columbia University**, USA.
[35] Williams, J. J. (1972) Augila field, Libya— Depositional environment and diagenesis of sedimentary reservoir and description of igneous reservoir: AAPG Memoir 16, **Society of Exploration Geophysicists** Special Publication 10, p. 623–632.
[36] Williams, J.J. (1971) Igneous and sedimentary reservoir rocks, Augila field, Libyan Arab Republic. First Symposium on the Geology of Libya (ed.) C. Gray. Faculty of Science, **University of Libya**, Tripoli, p. 501-512
[37] Wilson, M., and Guiraud R. (1998) Late Permian to Recent magmatic activity on the African-Arabian margin of Tethys, in D. S. Macgregor, R. T. J. Moody, and D. D. Clark-Lowes, (eds.) Petroleum geology of north Africa: **Geological Society** (London) Special Publication 132, p. 231–263.

Author Profile

Mohamed Saleem was born in Tripoli Libya in1960; in 1984 he under graduated in the geophysics engineering department at Tripoli University. In 1985, Mohamed joined the Libyan Baroid Company as a geological engineer, where he had gained a wide experience in the oil wells drilling operations and activities. In 1992 Mohamed joined the Libyan Petroleum Institute (LPI) formerly known Petroleum Research Centre (PRC) as an assistant researcher in the Exploration Dept. where he was involved in many research projects. In 2002, Mohamed started his postgraduate study in petroleum geosciences and management at the University of Manchester. After that he re-joined the Libyan Petroleum Institute, as a researcher, he was involved in a series of research studies and projects. In 2009, Mohamed started his Ph.D. research at the University of Birmingham, School of Geography, Earth and Environmental Sciences, and then he suspended his study for about 2 years due to the war events in Libya. In September 2012, he restarted his doctoral research, in October 2015 he has got his Ph.D. degree and

Licensed Under Creative Commons Attribution CC BY

joined the LPI again, in 2017 he became the manager of the Exploration Research department at Libyan Petroleum Institute.

Licensed Under Creative Commons Attribution CC BY